



pubsiacs.org/estwater Article

# Aqueous Elemental Mercury Production versus Mercury Inventories in the Lake Michigan Airshed: Deciphering the Spatial and Diel Controls of Mercury Gradients in Air and Water

Ryan F. Lepak,\* Michael T. Tate, Jacob M. Ogorek, John F. DeWild, Benjamin D. Peterson, James P. Hurley, and David P. Krabbenhoft



Cite This: https://dx.doi.org/10.1021/acsestwater.0c00187



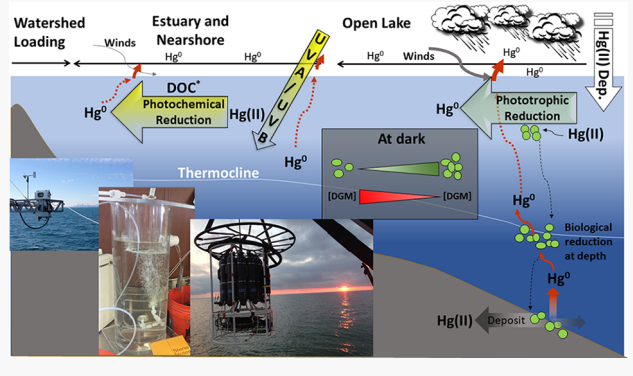
**ACCESS** 

Metrics & More

Article Recommendations

Supporting Information

**ABSTRACT:** Atmospheric delivery of mercury (Hg) is important to the Upper Great Lakes, and understanding gaseous Hg exchange between surface water and air is critical to predicting the effects of declining mercury emissions. Speciated atmospheric Hg, dissolved gaseous Hg (DGM), and particulate and filter passing total Hg were measured on a cruise in Lake Michigan. Low mercury levels reflected pristine background conditions, especially in offshore regions. In the atmosphere, reactive and particle-associated fractions were low (1.0  $\pm$  0.5%) compared to gaseous elemental Hg (1.34  $\pm$  0.14 ng m<sup>-3</sup>) and were elevated in the urbanized southern basin. DGM was supersaturated, ranging from 17.5  $\pm$  4.8 pg L<sup>-1</sup> (330  $\pm$  80%) in the main lake to  $33.2 \pm 2.4$  pg L<sup>-1</sup> (730  $\pm$  70%) in Green Bay. Diel cycling of surface DGM showed strong Hg efflux during the day due



to increased winds, and build-up at night from continued DGM production. Epilimnetic DGM is formed from photochemical reduction, while hypolimnetic DGM originates from biological Hg reduction. We found that DGM concentrations were greatest below the thermocline (30.8 ± 13.6 pg L<sup>-1</sup>), accounting for 68-92% of the total DGM in Lake Michigan, highlighting the importance of nonphotochemical reduction in deep stratified lakes.

KEYWORDS: dissolved gaseous mercury, microbes, photochemistry, redox cycling, Lake Guardian

# 1. INTRODUCTION

Mercury (Hg) is a ubiquitous and persistent pollutant capable of long-range atmospheric transport (residence time of 6-12 months) as gaseous elemental mercury (GEM), which can contaminate even remote regions of the world. Anthropogenic activities like mining, industrial and medical Hg applications, and coal combustion have altered the dominant sources of Hg worldwide and increased concentrations 4-6-fold above historic levels.<sup>2</sup> In the atmosphere, Hg undergoes reactions with oxidants, transforming GEM into reactive and watersoluble gaseous oxidized mercury (GOM), which is also susceptible to particle sorption [particle-bound mercury (PBM)]. Due to the long-range atmospheric transport of GEM and high deposition velocities of GOM and PBM species, aquatic ecosystems worldwide are exposed to Hg through direct atmospheric deposition (wet and dry) to the water surface and indirectly through watershed inputs.<sup>3–5</sup> Once GOM and PBM are deposited, water column processes result in Hg sedimentation, reduction to GEM [here called dissolved gaseous Hg (DGM)], partitioning to organic matter, and microbially mediated transformations of inorganic mercury to methylmercury.<sup>6</sup> Among the potential outcomes of the

deposition of Hg in aquatic systems, the microbial formation of neurotoxic methylmercury is of particular concern and a potential threat to aquatic ecosystems and human health.

Recent studies have shown that the removal of Hg in waste prior to incineration, air pollution control strategies (like SO<sub>x</sub> and NOx abatement), and the conversion from coal-fired power plants to natural gas have led to a roughly 40% reduction in Hg emissions in the United States. 7,8 Decreases in Hg emissions have resulted in changes in Hg cycling in the environment, evidence that is quantifiable in fish, water, and sediments, and is especially clear in the Laurentian Great Lakes where a large proportion of Hg delivered to the lakes is from atmospheric delivery pathways.

Once GOM and PBM enter aquatic ecosystems, a suite of redox reactions can occur by both abiotic and biotic reduction

Received: October 5, 2020 Revised: December 15, 2020 Accepted: December 16, 2020



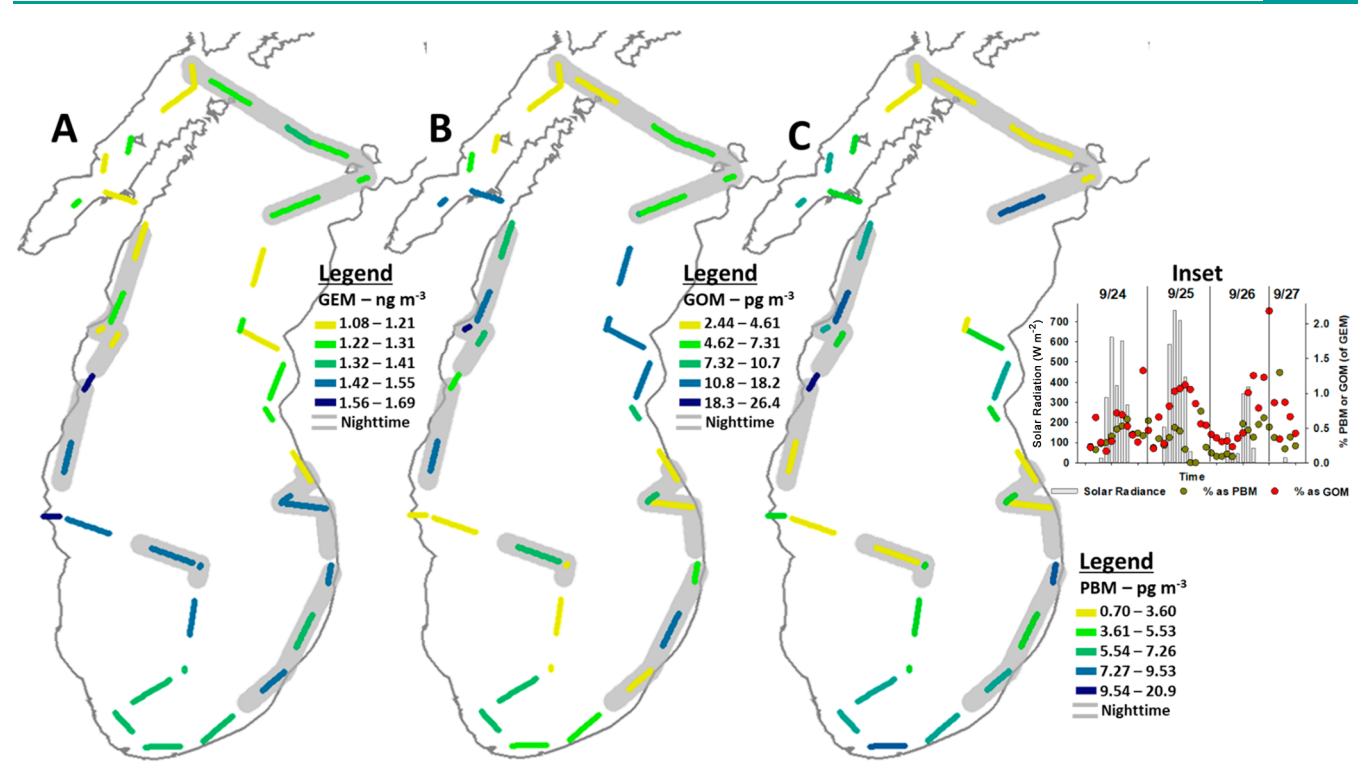


Figure 1. (A) Gaseous elemental Hg was collected in the atmosphere during the 2013 September cruise onboard the EPA *Lake Guardian* beginning in Milwaukee, WI, and traversing counterclockwise around the lake. Dashed lines indicate the average concentration observed over that transect. (B) Reactive oxidized Hg collected simultaneously with (C) particulate matter-bound Hg. Dashed lines indicate the average concentration observed over that transect and gray-scale over the transcet path indicates nighttime sampling. Dashed line colors indicate the average concentration observed over that transect. The inset shows the spatially aligned percent GOM or PBM of GEM. Gray bars represent the average solar radiation (watts per square meter) for that specific transect.

pathways, reducing the inorganic oxidized mercury back to DGM. Inorganic oxidized mercury can be photochemically reduced, a process that is mediated by dissolved carbon species acting as an electron donor or through light absorption. <sup>9–11</sup> In addition, direct and indirect (via the production of reductants) microbially mediated Hg reduction is important in freshwater lakes. <sup>12–15</sup> Finally, photoreduction mediated by manganese and iron is possible but is likely insignificant in Lake Michigan because the solubility of manganese and iron is low in the oxic water column. <sup>16–18</sup> Once formed, DGM may be reoxidized (cycling back to GOM and/or PBM) or leave the aquatic system entirely by evasive Hg flux. <sup>10,12,17,19,20</sup> Therefore, DGM measurements reflect net reduction rather than absolute production. Due to the low solubility of DGM in freshwater (5.1 pg L<sup>-1</sup> at 20 °C), it is often supersaturated, as calculated by Henry's law. <sup>9,16</sup>

$$(C_{\text{air}}K_{\text{h}})/C_{\text{water}} = \% \text{ saturation}$$
 (1)

where  $C_{\rm air}$  is the air GEM concentration,  $C_{\rm water}$  is the water DGM concentration, and  $K_{\rm h}$  is Henry's constant. The complex processes of reduction of deposited oxidized mercury and emission back to the atmosphere ultimately result in a significant loss of Hg to aquatic systems; we sought to investigate the relative importance of each in Lake Michigan following the large declines in Hg emissions and re-engineering of the water column from invasive mussels.

Many of the changes to Lake Michigan are common to the Great Lakes broadly, and to appropriately create a Hg mass balance for the Great Lakes, re-evaluation of Hg fluxes is necessary. Here we focus on the air-water flux of

elemental Hg in Lake Michigan, as well as the formation of DGM, through spatial, vertical, and diel lenses. We compare Hg flux to meteorological conditions (wind, temperature, and humidity) and DGM formation to biological, physical, limnological, and photochemical parameters to better understand atmospherically deposited mercury cycles in Lake Michigan. 16,24,25 We continuously measured DGM in Lake Michigan surface water while simultaneously measuring GEM, GOM, and PBM in the overlying airshed. At point locations, we also collected vertical profiles in nearshore and offshore regions, spanning a gradient of anthropogenic contamination, to provide a novel perspective on photochemical and microbial reduction processes. 11,17,26,27 Finally, we coupled these results with molecular dynamics to understand what physical and chemical processes influence Hg flux and compare the relative importance of biological and photochemical reduction processes in Lake Michigan. Additionally, we reveal the importance of wind-driven turbulence in driving Hg evasion. These efforts will help us better understand how the lake has responded to changes in energy flow<sup>28</sup> and Hg loading in recent decades.2

#### 2. EXPERIMENTAL METHODS

**2.1. Sampling Strategy.** While underway, we continuously measured GEM, GOM, PBM, and DGM in Lake Michigan while onboard the U.S. Environmental Protection Agency R/V *Lake Guardian* from September 23 to 29, 2013.<sup>29</sup> Figures 1 and 2 provide the sampling path (originating in Milwaukee, WI) that generally follows a counterclockwise progression. Throughout the mercury sampling, continuous

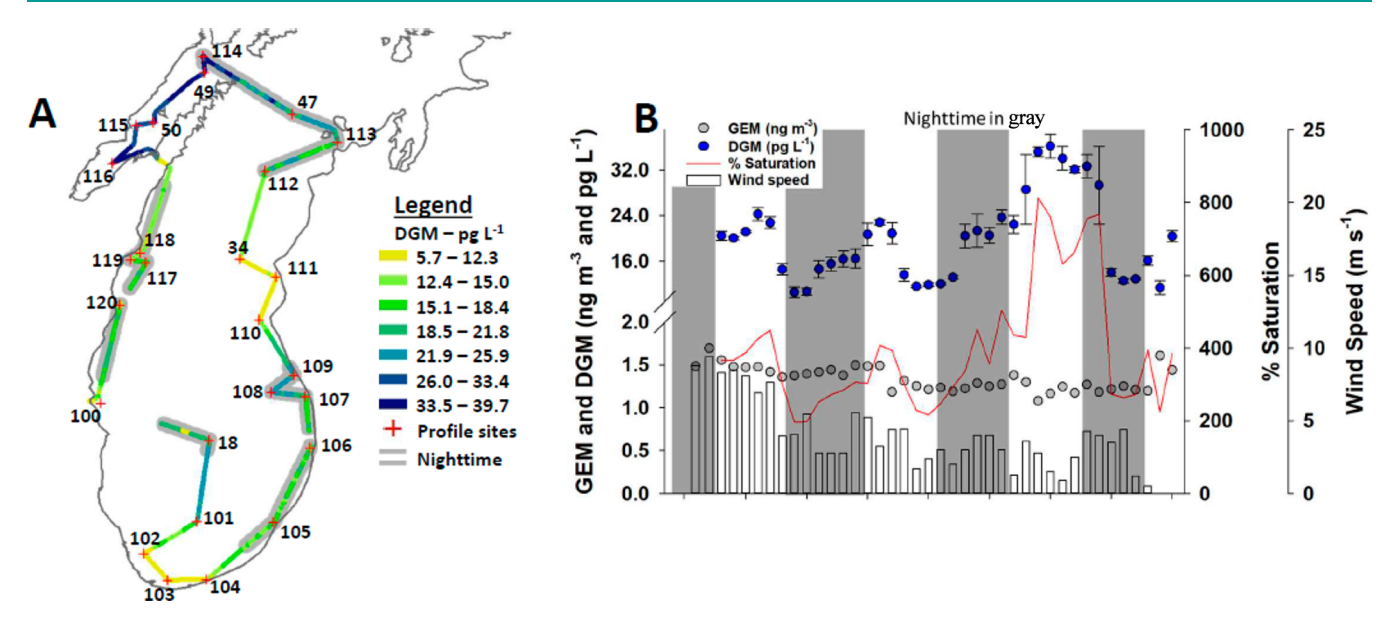


Figure 2. (A) Continuously measured surface dissolved gaseous Hg (picograms per liter) via the flow-through system during the 2013 September cruise onboard the EPA *Lake Guardian* beginning offshore from Milwaukee, WI, and traversing counterclockwise around the lake. (B) Averaged surface DGM (blue dots and one standard deviation) for each transect overlaid with a GEM transect value (gray dots) from Figure 1 A. The red line represents the percent saturation (calculated by Henry's law) for each step. Black outlined bars represent the average windspeed (meters per second) for that specific transect, and the gray shading indicates nighttime sampling.

measurements of wind speed, air temperature, GPS location, and surface water temperature were also taken (Tables S1 and S2). At discrete sites, the vessel was held stationary while water was collected in a vertical profile by remotely triggered trace metal clean Niskin bottles and analyzed for DGM, dissolved organic carbon (DOC), and filter passing total mercury (FHgT) (Table S3). At these locations, continuous DGM was also collected for comparative purposes (Figure S1). Water quality measurements were taken at the discrete sites, including temperature, chlorophyll *a*, turbidity, fluorescent dissolved organic matter, conductivity, and dissolved oxygen (Figures S2–S26). This allowed for operationally defined depth interval sampling (surface to 2 m from the air—water interface, midepilimnion, thermocline, midhypolimnion, and bottom to 2 m above sediments).

2.2. Atmospheric Hg Measurement. Speciated atmospheric Hg measurements were performed by the sequential application of Tekran instrumentation. Sample intake was through Teflon tubing, with the inlet located on an armature extending approximately 5 m off the bow of the ship. Tekran mercury speciation units 1130 and 1135 were used to separate the GOM and PBM from the atmospheric sample stream by capture onto a potassium chloride-coated annular denuder and regenerable quartz fiber filter (diameter of 22 mm), respectively. The remaining mercury in the atmospheric sample stream is GEM, which passes through the speciation units unchanged, and is analyzed at 5 min intervals by an automated cold vapor atomic fluorescence spectrophotometer (CVAFS, Tekran model 2537A). After a 60 min cycle of PBM and GOM collection and GEM analysis, the instrumentation is flushed with Hg-free air and the speciation units are heated, simultaneously desorbing and reducing PBM and GOM to elemental mercury that is detected<sup>30,31</sup> by CVAFS. Calibration was performed daily (did not exceed 2% from precampaign calibration) and is described elsewhere. 16

2.3. Continuous Surface DGM and Vertical DGM Profile Analysis. Surface water DGM was measured by

sparging Hg-free air through a continuous supply of surface water in a custom-designed 30 L flow-through vessel. The flow-through vessel was precleaned to trace metal conditions and constructed of a polyethylene terephthalate container and a quartz glass sparging interface. GEM concentrations in the equilibrated headspace of the flow-through vessel were measured using a Tekran 2537A CVAFS gaseous Hg analyzer, and DGM supersaturation was calculated from Henry's law. A method detection limit was estimated at approximately 3 pg L<sup>-1</sup>. This was determined by shutting off the water inflow until a constant GEM concentration was measured in the headspace.

Water samples were collected in profiles at discrete sample sites for DGM analysis in trace metal clean Niskin bottles. Upon collection, 1 L of water was immediately transferred into precleaned glass sparge vessels. Raw water samples (without chemical amendment) were sparged for 20 min (400 mL min<sup>-1</sup>) onboard the ship with ultrapure nitrogen. The resulting DGM was captured on gold traps, thermally desorbed, and analyzed by CVAFS detection. 33,34 Method detection limits were 3 pg L<sup>-1</sup>. To compare accuracy between the two DGM collection methods, results from the discrete sampling sites and the flow-through vessel were compared and were in good agreement ( $R^2 = 0.91$ ); however, at lower concentrations (<20 pg L<sup>-1</sup>), the manual method was biased high [35  $\pm$  13% difference (Figure S1)] when compared to flow-through methods; thus, DGM concentrations below 15 pg L<sup>-1</sup> should be treated as estimates.

**2.4. Mercury Flux Calculations.** At the air-water interface, the solubility of gases is dependent on the equilibrium distribution, while the magnitude and direction of exchange are dependent on multiple physical parameters, including wind speed, temperature, and, in the case of Hg, the presence or absence of light [primarily ultraviolet (UV)]. Flux (F) is calculated as the concentration difference between air and water ( $\Delta c^{\rm air-water}$ ) multiplied by the wind-corrected gas exchange transfer velocity ( $k_{\rm u}$ ):  $^{35,36}$ 

$$F = k_{\rm u} \Delta c^{\rm air-water} \tag{2}$$

To obtain more accurate and environmentally relevant values of  $k_{\rm u}$ , researchers developed a Schmidt model (Schmidt number, Sc) using molecular dynamics and empirical determinations for  ${\rm CO_2}$  in fresh water to better estimate flux over varying wind and temperature conditions. The adaptation from  ${\rm CO_2}$  to Hg includes considerations for the kinetic viscosity of fresh water  $(\nu)^{37}$  and the diffusivity of Hg (D).

$$Sc = \nu/D$$
 (3)

With this knowledge, a temperature-corrected  $k_{\rm u}$  can be calculated for Hg for gases:

$$k_{\rm u} = k_{600}(u) \left(\frac{Sc}{600}\right)^{-n} \tag{4}$$

where n=0.5 is the recommended correction term for environmental conditions  $^{37,38}$  and  $k_{600}(u)$  is the wind-dependent freshwater Schmidt number for  $CO_2$ . The relationship between  $Sc_{Hg}$  and  $Sc_{CO_2}$  was determined by a combination of gas transfer velocity and kinematic viscosity work developed elsewhere. The diffusion coefficient could ultimately be determined by

$$D = Ae^{-E_a/RT} (5)$$

where for Hg,  $E_a$  is 16.98 kJ mol<sup>-1</sup> for freshwater, A is 0.01768 cm<sup>2</sup> s<sup>-1</sup>, T is the temperature, and R is the ideal gas constant.

2.5. Multiple Regression. To determine which factors were most important in controlling DGM in Lake Michigan surface waters, we ran a multiple regression of the DGM values against measured parameters that are expected to influence DGM. Parameters included air-water DGM flux, total phytoplankton biomass, photosynthetic active radiation (PAR), surface temperature, GEM, and depositional Hg. Because flux, GEM, GOM, PBM, and DGM were all measured or calculated continuously and did not always overlap with the discrete sampling sites at which profiles were measured, we used an average of the measurements at each site location. We obtained meteorological conditions and wave data from closest Great Lakes Observing System buoy at the time interval of sampling. PBM and GOM are tightly correlated and are both thought to be major sources of net atmospheric Hg deposition to aquatic ecosystems, <sup>21,39,40</sup> so we combined the two measurements into depositional Hg to avoid overfitting our regressions.4 While GEM is a component of the DGM airwater gradient and thus a component in the flux calculations, flux is thought to be driven largely by wind speed, so we included both flux and GEM in the model but excluded wind speed. Water temperature, relative biomass (fluorescence), and PAR data were taken from the profiles collected at each site with data available from the Great Lake Environmental Database. Because the continuous surface DGM was collected approximately 2 m below the surface, we averaged the water quality parameters over the top 4 m for the multiple regressions. Biomass included four narrow bands of excitation and emission (intending to capture optical properties of four types of phytoplankton), some of which are important to Hg dynamics. 11,41,42 Green Bay sites were excluded from regressions due to the effect of Hg loading from the Fox River as well as extensive nutrient loading (leading to increased biomass) not present in most of the main lake. The multiple regression was calculated using R base functions (R version 3.2.2).<sup>43</sup>

#### 3. RESULTS AND DISCUSSION

3.1. Atmospheric GOM and PBM Concentrations. Together, GOM (0.37  $\pm$  0.24%) and PBM (0.66  $\pm$  0.42%) constituted on average 1.0  $\pm$  0.5% of the GEM signal (Figure 1, inset). Diel cycling of reactive and particle-associated fractions is clear (Figure 1, inset), indicating GOM and PBM species are formed during daylight hours. This diel pattern of oxidation is consistent with observations made previously, albeit our resulting concentrations are much lower and less temporally stable than previous results. 19 Mechanistically, Landis et al. 4,31 surmised that the diel cycling of atmospheric Hg was dependent on the oxidation of GEM to GOM by ozone, hydroxyl radicals, and hydrogen peroxide (primarily in cloudwater),<sup>31</sup> and the reduction of GOM to GEM by gaseous SO<sub>2</sub> and dissolved SO<sub>3</sub><sup>2-</sup>. Although GOM and PBM are only a minor fraction of the overall atmospheric Hg pool, it is considered the largest component of net dry deposition to aquatic ecosystems.<sup>4</sup> It is likely that most of the dry atmospheric deposition that is retained in the Great Lakes as aqueous Hg is from the GOM and PBM fractions, rather than from direct GEM deposition.

**3.2. GEM and DGM Surface Dynamics.** Overall, GEM concentrations were relatively constant over the course of the study  $(1.34 \pm 0.14 \text{ ng m}^{-3})$  and no obvious diel fluctuations were observed (Figure 2B). GEM concentrations were slightly higher in the Lake Michigan southern basin (0.23 ng m<sup>-3</sup>), likely reflecting the more urbanized airshed. Compared to recent efforts, GEM concentrations in our study are 25-45% lower than previous atmospheric levels, a trend that has been observed elsewhere in the Northern Hemisphere.

Overall DGM concentrations averaged 17.5  $\pm$  4.8 pg L<sup>-1</sup> in the main lake, roughly 40% lower than previous observations in the 1990s to early 2000s, <sup>25,33</sup> with no measurable difference between nearshore (without a localized riverine influence) and offshore regions. In Green Bay, a eutrophic region susceptible to very high loading of filter passing and particulate Hg from the Fox River (median unfiltered HgT concentration of 24.8 ng L<sup>-1</sup> with 93.6% particle bound), <sup>44</sup> higher DGM concentrations were found (33.2  $\pm$  2.4 pg L<sup>-1</sup>). DGM was consistently supersaturated in the surface layer at 329  $\pm$  84% in the main lake and 732  $\pm$  69% in Green Bay, <sup>45</sup> indicating continual reduction of inorganic oxidized Hg in the water column by direct UV-induced photochemical (mediated directly by DOC or initiated by excited DOC) <sup>9,10,26</sup> and microbial processes. <sup>12</sup>

Surface DGM was also temporally variable, with diel dependence of DGM loss during the day (Figure 2B), due to wind-driven flux. This diel observation differs from previous studies, where DGM increases during the day are attributed to increased solar radiation and corresponding increased photoreduction. 16,19,46 Phototrophic cells can also produce DGM during photosynthesis, which would also lead to increased DGM production during the day.<sup>47</sup> However, in our study, DGM concentrations increased overnight. DGM production here could be controlled by microbial Hg reduction using mercuric reductase (mer operon), which is a dark aerobic reaction.<sup>48</sup> While high levels of Hg are required to induce mer expression, basal levels of mercuric reductase have been shown to be sufficient to reduce Hg<sup>49</sup> even at low levels. Lower DGM levels during the day could also be due to increased Hg flux rather than lower DGM production. Microbial oxidases that can oxidize DGM are produced in response to  $H_2O_2$ , which

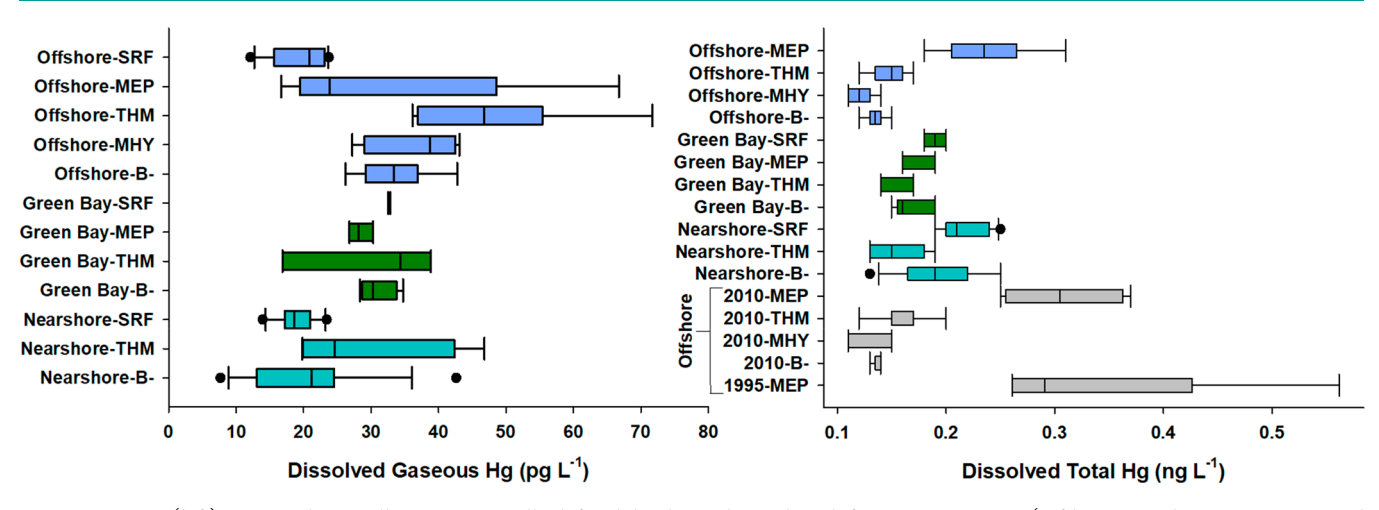


Figure 3. DGM (left) measured vertically at operationally defined depths. Color coding differentiates site type (offshore, nearshore, Green Bay, and offshore data from previous work). Inner box lines represent data median. Box edges represent 25th and 75th percentiles. Edges of the whiskers represent the 10th and 90th percentiles. Dots represent outliers (Sigmaplot 13). FHgT concentrations (right) over the same depth intervals and data from the literature (gray). <sup>24,25,28,33</sup>

builds up during daylight hours.<sup>12,13</sup> Additionally, DGM evasion from the surface water is likely to decrease at nighttime, when winds are weaker. Here we estimated daytime DGM production rates to be 0.9–1.2 pg L<sup>-1</sup> h<sup>-1</sup>, but DGM losses as evasive flux are 1.4–1.7 pg L<sup>-1</sup> h<sup>-1</sup>, confirming DGM losses exceed production during the day. These estimates and the supersaturation of DGM in the water column suggest Lake Michigan is continually undergoing evasive flux of Hg to the atmosphere. In the eutrophic Green Bay basin, it is likely that reduction of oxidized mercury by phototrophic microbes in the epilimnion is even greater than in pelagic Lake Michigan.<sup>50</sup> In addition, Green Bay is warmer and contains highly Hg contaminated sediment, which may further enhance DGM formation and supersaturation,<sup>51</sup> which is twice that compared to the value in the main body of Lake Michigan.

Unlike previous research, no relationship was observed between flux and percent saturation, 16 highlighting the significance of wind as a transport vector of Hg from Lake Michigan waters to the atmosphere. When a wind speed of 5 m s<sup>-1</sup> was used as a breakpoint in data models, fluxes were 0.60  $\pm$ 0.36 ng m<sup>-2</sup> h<sup>-1</sup> (25  $\pm$  15 kg month<sup>-1</sup>) and 2.96  $\pm$  1.23 ng  $m^{-2}$   $h^{-1}$  (125 ± 52 kg month<sup>-1</sup>) for low- and high-wind conditions, respectively, with the value for the lower-wind conditions being similar to previous findings in Lake Michigan (~21 kg month<sup>-1</sup>),<sup>33</sup> but higher than those of the Atlantic Ocean. 52 These fluxes are also comparable to those from a similar study investigating Lake Ontario where median flux was estimated to be 2.88 ng  $\mbox{m}^{-2}~\mbox{h}^{-1}$  and percent saturation ranged from 476% to 2,163%. Ontario fluxes are most likely higher due to increased FHgT water concentrations, which average 100-200 pg L<sup>-1</sup> higher than in Lake Michigan (200-400 pg L<sup>-1</sup>). Sediment Hg concentrations are also an order of magnitude higher in Lake Ontario, which likely further increases the DGM concentrations.  $^{24,25,51,53}$ 

Our multiple-regression data model showed that GEM, depositional Hg, biomass, and temperature had no effect on DGM, while flux does influence DGM concentrations (p = 0.005). We also observe that PAR significantly impacted DGM concentrations (p = 0.016), but unlike other studies, this was a negative correlation. He cause PAR at the surface can predict UV light intensity, which is expected to reduce Hg in circumneutral conditions, we would expect to see a positive

correlation between PAR and DGM levels. One potential explanation is the correlation between wind and PAR during the daytime. Potentially, this counterintuitive result also signals a lag in the production of photooxidants because DGM production continues into the night. Because Lake Michigan DOC is fairly homogeneous in concentration (2–3 mg L $^{-1}$ ) and spectral character (more photo-oxidized),  $^{40,54}$  we do not suspect that variance in DOC drives the variance in DGM formation or flux but do acknowledge it plays a critical role in the Hg reduction process.  $^{10,17,27,55}$ 

3.3. Vertical Profiles of DGM and Associated Water Quality Characteristics. To better understand water column dynamics and formation of DGM, vertical profiles were collected at multiple sites. Connecting the biological and physical limnology of the lake allows for better resolution of the impact of phytoplankton on DGM formation. Vertical profiles of temperature, fluorescence for phototrophic pigments, PAR, and dissolved oxygen, combined with the resulting DGM concentration profiles, show that a strong separation between the epilimnion and hypolimnion exists for offshore sites, while mixed water columns are evident in nearshore sites and Green Bay (see SI). In addition, the thermocline generally becomes shallower with an increase in latitude, likely due to the generally cooler atmosphere. Where available, NOAA monitoring buoys confirmed the temporal stability of these thermal structures.

To compare DGM and FHgT concentrations of similar water parcels in Lake Michigan, we used water temperature to separate the layers of water at stratified sites and grouped sites by location [nearshore, offshore, and Green Bay (Figure 3)]. For each layer at all sites, the DGM concentrations were supersaturated in water. Even in the main lake where dissolved oxygen levels were at or near the point of saturation, DGM production was occurring. DGM concentrations in the thermocline, hypolimnion, and benthic layers were elevated relative to the surface layer, despite lacking the potential for photochemical reduction. Deeper waters were lower in dissolved Hg than the surface counterparts, <sup>24,25,28,40</sup> eliminating the possibility that sediment-FHgT efflux was resulting in increased DGM concentrations. We did not observe clear evidence that sediment-formed DGM and subsequent DGM diffusion and accumulation at the thermocline was the primary

mechanism for hypolimnetic DGM because benthic waters lacked convincing increases in DGM concentration relative to directly overlying water. In Green Bay, the high DGM percent saturation (ranging from 400% to 800%) is due to increased sediment Hg, <sup>53</sup> and increased microbial reduction due to eutrophication and increased biological oxygen demand <sup>50</sup> that support anoxia. The weakly stratified nearshore regions had the largest and most variable DGM at the midwater column thermocline. We also noted that the large variation in DGM concentrations at the midepilimnion and thermocline of the main lake coincided with increases in the relative fluorescence (tracing organic molecules and biological productivity) of the water profile.

Increased DGM concentrations in the thermocline and hypolimnion likely reflect the capture of microbially produced DGM below the thermocline in the oxic water column that cannot evade and is lost to only reoxidation or sorption. Only a modest amount of mixing occurs across the thermocline, and the midhypolimnion and benthic regions are absent of photochemical reduction;<sup>40</sup> therefore, Hg reduction is likely biotic at depth. Bacterial mercuric reductases (mer operon) are active under oxic conditions at lower efficiencies due to basal levels of expression of the mer operon under environmental conditions. 66 Other studies have pointed to phytoplankton biomass, rather than bacterial mer activity, as driving biotic DGM reduction, 11,41,42,57 which is consistent with the increased DGM levels coincident with peaks in photosynthetic pigments. Additionally, one study suggested the production of DGM was not directly linked to photosynthesis but rather to intracellular reduction processes or to the excretion of reductants into the surrounding water. <sup>11</sup> We hypothesize that Hg reduction by primary producers is the dominant production pathway for DGM in the thermocline where we see elevated levels of primary production and that deeper hypolimnetic DGM is primarily mediated by mercuric reductase.

To isolate the direct or indirect effect of phytoplankton on DGM dynamics in the presence or absence of light, we separated sampling depths from the main lake where the PAR values were 0, which included nighttime and samples at depth, from surface samples taken during the day. Samples in the dark included four nighttime surface samples and 31 samples from the thermocline or hypolimnion. We then summed the relative fluorescence units for measured wavelengths for green algae, blue green algae (cyanobacteria), diatoms, and cryptophyta and assumed it represents total measured phytoplankton fluorescence. In surface samples with detectable PAR values, there is a positive correlation between total phytoplankton fluorescence and DGM (Figure 4A). Surprisingly, we found a negative correlation between DGM concentrations and total phytoplankton fluorescence under dark conditions (Figure 4B). This supports our previously stated hypothesis that photosynthesis can help drive DGM production in surface waters, which is consistent with previous work. 11,57 Our results suggest the production of DGM by phototrophs stops at night with the cessation of photosynthesis, which is consistent with previous work that observed both lower DGM levels in phytoplankton layers under oligotrophic conditions and the cessations of DGM production when photosynthesis was inhibited. 11,41,42 However, the negative correlation between phytoplankton and DGM levels under dark conditions is unexpected and may suggest phototrophs are sorbing or reoxidizing DGM under dark conditions, as they cease

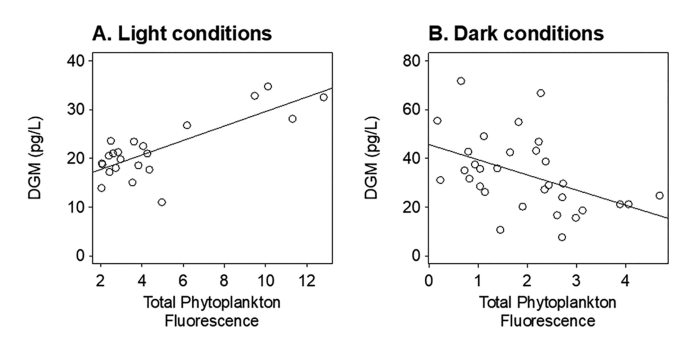


Figure 4. Total phytoplankton correlated (A) positively to DGM levels under light conditions and (B) negatively to DGM levels under dark conditions. Only samples with undetectable PAR readings were used to isolate DGM levels from photoreduction by solar radiance and as a byproduct of photosynthesis. Green Bay sites were excluded. Linear regressions were run for DGM against total phytoplankton under both conditions, and the resulting equations are plotted on their respective graphs. The equations and p values are as follows. Light conditions: 1.483X + 14.756; p < 0.0001. Dark conditions: -6.21X + 45.59; p = 0.010.

photosynthesis. Further investigation is necessary to understand the role of phytoplankton in DGM cycling of the hypolimnion and nighttime photic zone.

#### 4. CONCLUSIONS

These results are consistent with those found in the literature suggesting that aquatic systems are mostly supersaturated with DGM. While Hg reduction pathways may result in excess DGM, another consideration may include the realization that the Henry's law coefficients and fundamental understanding of the solubility of elemental Hg are difficult to apply. This is the first work known to include the molecular dynamics considerations proposed by Kuss et al.<sup>38</sup> that incorporates a temperature- and wind-specific consideration into the Schmidt number for Hg to freshwater. Typically, regressions from CO<sub>2</sub> values have been used, dramatically increasing the calculated flux (as much as 20%).<sup>38</sup> Surface water data indicate that for Lake Michigan, the most important factor controlling DGM level is the air-water elemental Hg flux, which is largely controlled by wind speeds. This contrasts with several other studies in which solar radiance controlled DGM levels by photoreduction. Phototrophs under light conditions correlated positively with DGM levels, suggesting that phototrophic activity can drive DGM formation. However, we observed an unexpected negative correlation between phytoplankton abundance and DGM levels under dark conditions, suggesting that there may be additional and unexplored factors influencing DGM cycling. Within the main lake (not including Green Bay), we found that DGM concentrations were greatest below the thermocline while FTHg concentrations were greatest in the epilimnion. The zone where photochemical reduction by UV light is most likely, the upper 7 m, 40 accounts for only 3–9% of the total DGM in main basin Lake Michigan (33–39% in Green Bay). When we include the entire euphotic zone, defined as the water surface to 26.3 m, 40 we can account for 9-32% of all DGM in main basin Lake Michigan, so >70% of the 140-170 kg of DGM in main basin Lake Michigan is produced by nonphotochemical reduction processes that we believe to be related to biological reduction. While clearing waters from invasive mussels has changed Hg cycling dynamics,<sup>28</sup> we do not hypothesize that the increased amount

of photochemical Hg reduction resulted in the lower Hg levels measured in Lake Michigan. Instead, our observed decreases in FHgT and DGM in the water column relative to the late 1990s and early 2000s<sup>4,24,25,33</sup> likely provide confidence that reductions in atmospheric Hg<sup>8</sup> are translating to reductions in water column Hg of the Great Lakes, a testament to the local and regional benefits of domestic regulations on Hg releases in the United States.

# ASSOCIATED CONTENT

# Supporting Information

The Supporting Information is available free of charge at https://pubs.acs.org/doi/10.1021/acsestwater.0c00187.

Additional text, analytical method comparisons, vertical water chemistry profiles at point locations, satellite imagery of Lake Michigan for the cruise dates, and relevant data tables (PDF)

## AUTHOR INFORMATION

### **Corresponding Author**

Ryan F. Lepak — Environmental Chemistry and Technology Program, University of Wisconsin-Madison, Madison, Wisconsin 53706, United States; Upper Midwest Water Science Center, USGS Mercury Research Laboratory, U.S. Geological Survey, Middleton, Wisconsin 53562, United States; Center for Computational Toxicology and Exposure, Great Lakes Toxicology and Ecology Division, U.S. EPA Office of Research and Development, Duluth, Minnesota 55804, United States; orcid.org/0000-0003-2806-1895; Email: rlepak@wisc.edu

# **Authors**

Michael T. Tate – Upper Midwest Water Science Center, USGS Mercury Research Laboratory, U.S. Geological Survey, Middleton, Wisconsin 53562, United States

Jacob M. Ogorek – Upper Midwest Water Science Center, USGS Mercury Research Laboratory, U.S. Geological Survey, Middleton, Wisconsin 53562, United States

John F. DeWild – Upper Midwest Water Science Center, USGS Mercury Research Laboratory, U.S. Geological Survey, Middleton, Wisconsin 53562, United States

Benjamin D. Peterson — Environmental Chemistry and Technology Program, University of Wisconsin-Madison, Madison, Wisconsin 53706, United States

James P. Hurley – Environmental Chemistry and Technology Program, University of Wisconsin–Madison, Madison, Wisconsin 53706, United States; University of Wisconsin Aquatic Sciences Center, Madison, Wisconsin 53706, United States; Occid.org/0000-0003-4430-5319

David P. Krabbenhoft — Upper Midwest Water Science Center, USGS Mercury Research Laboratory, U.S. Geological Survey, Middleton, Wisconsin 53562, United States; orcid.org/0000-0003-1964-5020

Complete contact information is available at: https://pubs.acs.org/10.1021/acsestwater.0c00187

## **Author Contributions**

M.T.T. and D.P.K. designed the study. R.F.L. and M.T.T. wrote this manuscript. M.T.T., J.M.O., J.F.D., D.P.K., B.D.P., J.P.H., and R.F.L. provided samples and provided substantial field and analytical support. J.M.O., D.P.K., and J.P.H. provided editorial comments.

#### Notes

The authors declare no competing financial interest.

#### ACKNOWLEDGMENTS

The authors gratefully acknowledge the U.S. EPA's Great Lakes National Program Office for funding support and extensive time granted onboard the research vessel Lake Guardian. The authors thank the crew of the research vessel Lake Guardian for their assistance and program coordinators Elizabeth Murphy and Ted Smith. This work benefited greatly from the long-term support to the USGS Mercury Research Lab by the USGS Toxic Substances Hydrology Program. Partial graduate student support was provided by the Wisconsin Alumni Research Foundation through the University of Wisconsin-Madison Graduate School (Grant MSN165161), and the University of Wisconsin Water Resources Institute through a USGS-NIWR fellowship (Grant MSN197848). Postdoctoral support was provided by the National Science Foundation Postdoctoral Fellowships for Research in Biology-Collection Program 2018 (Grant 1812211). We also thank Dr. Galen McKinley who inspired concepts within this manuscript through her teaching. The authors thank internal reviewers for providing a volunteer peer review of this work and its findings. The authors thank the anonymous reviewers whose valuable comments and suggestions helped to improve the manuscript.

#### REFERENCES

- (1) Zhu, W.; Lin, C.-J.; Wang, X.; Sommar, J.; Fu, X.; Feng, X. Global observations and modeling of atmosphere-surface exchange of elemental mercury: a critical review. *Atmos. Chem. Phys.* **2016**, *16* (7), 4451–4480.
- (2) Hsu-Kim, H.; Kucharzyk, K. H.; Zhang, T.; Deshusses, M. A. Mechanisms regulating mercury bioavailability for methylating microorganisms in the aquatic environment: a critical review. *Environ. Sci. Technol.* **2013**, 47 (6), 2441–2456.
- (3) Hurley, J. P.; Cowell, S. E.; Shafer, M. M.; Hughes, P. E. Tributary loading of mercury to Lake Michigan: Importance of seasonal events and phase partitioning. *Sci. Total Environ.* **1998**, 213 (1–3), 129–137.
- (4) Landis, M. S.; Keeler, G. J. Atmospheric mercury deposition to Lake Michigan during the Lake Michigan mass balance study. *Environ. Sci. Technol.* **2002**, 36 (21), 4518–4524.
- (5) Marvin, C. H.; Charlton, M. N.; Reiner, E. J.; Kolic, T.; MacPherson, K.; Stern, G. A.; Braekevelt, E.; Estenik, J.; Thiessen, L.; Painter, S. Surficial sediment contamination in Lakes Erie and Ontario: A comparative analysis. *J. Great Lakes Res.* **2002**, 28 (3), 437–450.
- (6) Ullrich, S. M.; Tanton, T. W.; Abdrashitova, S. A. Mercury in the aquatic environment: a review of factors affecting methylation. *Crit. Rev. Environ. Sci. Technol.* **2001**, *31* (3), 241–293.
- (7) Selin, N. E. Global change and mercury cycling: Challenges for implementing a global mercury treaty. *Environ. Toxicol. Chem.* **2014**, 33 (6), 1202–1210.
- (8) Zhang, Y.; Jacob, D. J.; Horowitz, H. M.; Chen, L.; Amos, H. M.; Krabbenhoft, D. P.; Slemr, F.; St. Louis, V. L.; Sunderland, E. M. Observed decrease in atmospheric mercury explained by global decline in anthropogenic emissions. *Proc. Natl. Acad. Sci. U. S. A.* **2016**, *113* (3), 526–531.
- (9) Garcia, E.; Amyot, M.; Ariya, P. A. Relationship between DOC photochemistry and mercury redox transformations in temperate lakes and wetlands. *Geochim. Cosmochim. Acta* **2005**, *69* (8), 1917–1924.
- (10) O'driscoll, N.; Siciliano, S.; Lean, D.; Amyot, M. Gross photoreduction kinetics of mercury in temperate freshwater lakes and rivers: application to a general model of DGM dynamics. *Environ. Sci. Technol.* **2006**, *40* (3), 837–843.

- (11) Poulain, A.; Amyot, M.; Findlay, D.; Telor, S.; Barkay, T.; Hintelmann, H. Biological and photochemical production of dissolved gaseous mercury in a boreal lake. *Limnol. Oceanogr.* **2004**, *49* (6), 2265–2275.
- (12) Siciliano, S. D.; O'Driscol, N. J.; Lean, D. Microbial reduction and oxidation of mercury in freshwater lakes. *Environ. Sci. Technol.* **2002**, *36* (14), 3064–3068.
- (13) Smith, T.; Pitts, K.; McGarvey, J. A.; Summers, A. O. Bacterial oxidation of mercury metal vapor, Hg (0). *Appl. Environ. Microbiol.* **1998**, *64* (4), 1328–1332.
- (14) Rolfhus, K. R; Fitzgerald, W. F The evasion and spatial/temporal distribution of mercury species in Long Island Sound, CT-NY. *Geochim. Cosmochim. Acta* **2001**, *65*, 407–418.
- (15) Rolfhus, K. R.; Fitzgerald, W. F. Mechanisms and temporal variability of dissolved gaseous mercury production in coastal seawater. *Mar. Chem.* **2004**, *90* (1–4), 125–136.
- (16) Poissant, L.; Amyot, M.; Pilote, M.; Lean, D. Mercury water-air exchange over the upper St. Lawrence River and Lake Ontario. *Environ. Sci. Technol.* **2000**, 34 (15), 3069–3078.
- (17) Zhang, H.; Lindberg, S. E. Sunlight and iron (III)-induced photochemical production of dissolved gaseous mercury in freshwater. *Environ. Sci. Technol.* **2001**, 35 (5), 928–935.
- (18) Chadwick, S. P.; Babiarz, C. L.; Hurley, J. P.; Armstrong, D. E. Influences of iron, manganese, and dissolved organic carbon on the hypolimnetic cycling of amended mercury. *Sci. Total Environ.* **2006**, 368 (1), 177–188.
- (19) Lindberg, S.; Meyers, T.; Munthe, J. Evasion of mercury vapor from the surface of a recently limed acid forest lake in Sweden. *Water, Air, Soil Pollut.* **1995**, *85* (2), 725–730.
- (20) Poissant, L.; Casimir, A. Water-air and soil-air exchange rate of total gaseous mercury measured at background sites. *Atmos. Environ.* **1998**, 32 (5), 883–893.
- (21) Lepak, R. F.; Hoffman, J. C.; Janssen, S. E.; Krabbenhoft, D. P.; Ogorek, J. M.; DeWild, J. F.; Tate, M. T.; Babiarz, C. L.; Yin, R.; Murphy, E. W.; et al. Mercury source changes and food web shifts alter contamination signatures of predatory fish from Lake Michigan. *Proc. Natl. Acad. Sci. U. S. A.* **2019**, *116* (47), 23600–23608.
- (22) Zhou, C.; Cohen, M. D.; Crimmins, B. A.; Zhou, H.; Johnson, T. A.; Hopke, P. K.; Holsen, T. M. Mercury temporal trends in top predator fish of the Laurentian Great Lakes from 2004 to 2015: are concentrations still decreasing? *Environ. Sci. Technol.* **2017**, *51* (13), 7386–7394.
- (23) Barbiero, R. P.; Lesht, B. M.; Hinchey, E. K.; Nettesheim, T. G. A brief history of the US EPA Great Lakes National Program Office's water quality survey. *J. Great Lakes Res.* **2018**, 44 (4), 539–546.
- (24) Mason, R. P.; Sullivan, K. A. Mercury in lake Michigan. *Environ. Sci. Technol.* **1997**, *31* (3), 942–947.
- (25) Sullivan, K. A.; Mason, R. P. The concentration and distribution of mercury in Lake Michigan. *Sci. Total Environ.* **1998**, 213 (1–3), 213–228.
- (26) Amyot, M.; McQueen, D. J.; Mierle, G.; Lean, D. R. Sunlight-induced formation of dissolved gaseous mercury in lake waters. *Environ. Sci. Technol.* **1994**, 28 (13), 2366–2371.
- (27) O'Driscoll, N.; Siciliano, S.; Lean, D. Continuous analysis of dissolved gaseous mercury in freshwater lakes. *Sci. Total Environ.* **2003**, 304 (1–3), 285–294.
- (28) Lepak, R. F.; Krabbenhoft, D. P.; Ogorek, J. M.; Tate, M. T.; Bootsma, H. A.; Hurley, J. P. Influence of cladophora-quagga mussel assemblages on nearshore methylmercury production in Lake Michigan. *Environ. Sci. Technol.* **2015**, *49* (13), 7606–7613.
- (29) Lenaker, P. L.; Corsi, S. R.; Mason, S. A. Spatial Distribution of Microplastics in Surficial Benthic Sediment of Lake Michigan and Lake Erie. *Environ. Sci. Technol.* **2020**, DOI: 10.1021/acs.est.0c06087.
- (30) Bloom, N.; Fitzgerald, W. F. Determination of volatile mercury species at the picogram level by low-temperature gas chromatography with cold-vapour atomic fluorescence detection. *Anal. Chim. Acta* 1988, 208, 151–161.
- (31) Landis, M. S.; Stevens, R. K.; Schaedlich, F.; Prestbo, E. M. Development and characterization of an annular denuder method-

- ology for the measurement of divalent inorganic reactive gaseous mercury in ambient air. *Environ. Sci. Technol.* **2002**, *36* (13), 3000–3009.
- (32) Andersson, M. E.; Gårdfeldt, K.; Wängberg, I. A description of an automatic continuous equilibrium system for the measurement of dissolved gaseous mercury. *Anal. Bioanal. Chem.* **2008**, 391 (6), 2277.
- (33) Jeremiason, J. D.; Kanne, L. A.; Lacoe, T. A.; Hulting, M.; Simcik, M. F. A comparison of mercury cycling in Lakes Michigan and Superior. *J. Great Lakes Res.* **2009**, 35 (3), 329–336.
- (34) Rolfhus, K.; Sakamoto, H.; Cleckner, L.; Stoor, R.; Babiarz, C.; Back, R.; Manolopoulos, H.; Hurley, J. Distribution and fluxes of total and methylmercury in Lake Superior. *Environ. Sci. Technol.* **2003**, *37* (5), 865–872.
- (35) Liss, P. S.; Slater, P. G. Flux of gases across the air-sea interface. *Nature* **1974**, 247, 181–184.
- (36) Wilke, C.; Chang, P. Correlation of diffusion coefficients in dilute solutions. AIChE J. 1955, 1 (2), 264–270.
- (37) Nightingale, P. D.; Malin, G.; Law, C. S.; Watson, A. J.; Liss, P. S.; Liddicoat, M. I.; Boutin, J.; Upstill-Goddard, R. C. In situ evaluation of air-sea gas exchange parameterizations using novel conservative and volatile tracers. *Global Biogeochemical Cycles* **2000**, 14 (1), 373–387.
- (38) Kuss, J.; Holzmann, J. r.; Ludwig, R. An elemental mercury diffusion coefficient for natural waters determined by molecular dynamics simulation. *Environ. Sci. Technol.* **2009**, 43 (9), 3183–3186.
- (39) Harris, R. C.; Rudd, J. W.; Amyot, M.; Babiarz, C. L.; Beaty, K. G.; Blanchfield, P. J.; Bodaly, R.; Branfireun, B. A.; Gilmour, C. C.; Graydon, J. A.; et al. Whole-ecosystem study shows rapid fish-mercury response to changes in mercury deposition. *Proc. Natl. Acad. Sci. U. S. A.* 2007, 104 (42), 16586–16591.
- (40) Lepak, R. F.; Janssen, S. E.; Yin, R.; Krabbenhoft, D. P.; Ogorek, J. M.; DeWild, J. F.; Tate, M. T.; Holsen, T. M.; Hurley, J. P. Factors Affecting Mercury Stable Isotopic Distribution in Piscivorous Fish of the Laurentian Great Lakes. *Environ. Sci. Technol.* **2018**, *52* (5), 2768–2776.
- (41) Baeyens, W. a.; Leermakers, M. Elemental mercury concentrations and formation rates in the Scheldt estuary and the North Sea. *Mar. Chem.* **1998**, *60* (3–4), 257–266.
- (42) Mason, R.; Morel, F. M.; Hemond, H. The role of microorganisms in elemental mercury formation in natural waters. *Water, Air, Soil Pollut.* **1995**, 80 (1–4), 775–787.
- (43) R: A language and environment for statistical computing; R Foundation for Statistical Computing: Vienna, 2019.
- (44) Hurley, J. P.; Cowell, S. E.; Shafer, M. M.; Hughes, P. E. Partitioning and transport of total and methyl mercury in the lower Fox River, Wisconsin. *Environ. Sci. Technol.* **1998**, 32 (10), 1424–1432
- (45) Andersson, M. E.; Gårdfeldt, K.; Wängberg, I.; Strömberg, D. Determination of Henry's law constant for elemental mercury. *Chemosphere* **2008**, 73 (4), 587–592.
- (46) Krabbenhoft, D. P.; Hurley, J. P.; Olson, M. L.; Cleckner, L. B. Diel variability of mercury phase and species distributions in the Florida Everglades. *Biogeochemistry* **1998**, *40* (2–3), 311–325.
- (47) Grégoire, D. S.; Poulain, A. A little bit of light goes a long way: the role of phototrophs on mercury cycling. *Metallomics* **2014**, *6* (3), 396–407.
- (48) Barkay, T.; Miller, S. M.; Summers, A. O. Bacterial mercury resistance from atoms to ecosystems. *FEMS microbiology reviews* **2003**, 27 (2–3), 355–384.
- (49) Yu, H.; Chu, L.; Misra, T. K. Intracellular inducer Hg2+concentration is rate determining for the expression of the mercury-resistance operon in cells. *Journal of bacteriology* **1996**, *178* (9), 2712–2714.
- (50) Lin, P.; Klump, J. V.; Guo, L. Dynamics of dissolved and particulate phosphorus influenced by seasonal hypoxia in Green Bay, Lake Michigan. *Sci. Total Environ.* **2016**, *541*, 1070–1082.
- (51) Yin, R.; Lepak, R. F.; Krabbenhoft, D. P.; Hurley, J. P. Sedimentary records of mercury stable isotopes in Lake Michigan. *Elementa: Science of the Anthropocene* **2016**, *4*, 000086.

- (52) Andersson, M. E.; Sommar, J.; Gårdfeldt, K.; Jutterström, S. Air-sea exchange of volatile mercury in the North Atlantic Ocean. *Mar. Chem.* **2011**, *125* (1–4), 1–7.
- (53) Lepak, R. F.; Yin, R.; Krabbenhoft, D. P.; Ogorek, J. M.; DeWild, J. F.; Holsen, T. M.; Hurley, J. P. Use of stable isotope signatures to determine mercury sources in the Great Lakes. *Environ. Sci. Technol. Lett.* **2015**, 2 (12), 335–341.
- (54) Zhou, Z.; Guo, L.; Minor, E. C. Characterization of bulk and chromophoric dissolved organic matter in the Laurentian Great Lakes during summer 2013. *J. Great Lakes Res.* **2016**, 42 (4), 789–801.
- (55) O'Driscoll, N. J.; Vost, E.; Mann, E.; Klapstein, S.; Tordon, R.; Lukeman, M. Mercury photoreduction and photooxidation in lakes: Effects of filtration and dissolved organic carbon concentration. *J. Environ. Sci.* **2018**, *68*, 151–159.
- (56) Schaefer, J. K.; Letowski, J.; Barkay, T. mer-mediated resistance and volatilization of Hg (II) under anaerobic conditions. *Geomicrobiol. J.* **2002**, *19* (1), 87–102.
- (57) Kritee, K.; Motta, L. C.; Blum, J. D.; Tsui, M. T.-K.; Reinfelder, J. R. Photomicrobial visible light-induced magnetic mass independent fractionation of mercury in a marine microalga. ACS Earth and Space Chemistry 2018, 2 (5), 432–440.